

Scf Represses Cardiomyogenesis in Prospective Hemogenic Endothelium and Endocardium

Ben Van Handel,^{1,12} Amélie Montel-Hagen,^{1,12} Rajkumar Sasidharan,¹ Haruko Nakano,¹ Roberto Ferrari,² Cornelis J. Boogerd,^{8,9} Johann Schredelseker,¹ Yanling Wang,¹ Sean Hunter,¹ Tönis Org,¹ Jian Zhou,³ Xinmin Li,³ Matteo Pellegrini,^{1,4,5,6} Jau-Nian Chen,¹ Stuart H. Orkin,^{10,11} Siavash K. Kurdistani,^{2,4,5,6} Sylvia M. Evans,^{8,9} Atsushi Nakano,^{1,4,5,6} and Hanna K.A. Mikkola^{1,4,5,6,7,*}

¹Department of Molecular, Cell, and Developmental Biology

²Department of Biological Chemistry

³Department of Pathology and Laboratory Medicine

⁴Jonsson Comprehensive Cancer Center

⁵Molecular Biology Institute

⁶Eli and Edythe Broad Center of Regenerative Medicine and Stem Cell Research

⁷Department of Microbiology, Immunology, and Molecular Genetics

University of California, Los Angeles, Los Angeles, CA 90095, USA

⁸Skaggs School of Pharmacy and Pharmaceutical Sciences

⁹Department of Medicine

University of California, San Diego, La Jolla, CA 92093, USA

¹⁰Division of Hematology/Oncology, Children's Hospital and Dana-Farber Cancer Institute, Harvard Medical School, Boston, MA 02115, USA

¹¹Howard Hughes Medical Institute, Children's Hospital Boston, MA 02115, USA

¹²These authors contributed equally to this work

*Correspondence: hmikkola@mcdb.ucla.edu

<http://dx.doi.org/10.1016/j.cell.2012.06.026>

SUMMARY

Endothelium in embryonic hematopoietic tissues generates hematopoietic stem/progenitor cells; however, it is unknown how its unique potential is specified. We show that transcription factor Scf/Tal1 is essential for both establishing the hematopoietic transcriptional program in hemogenic endothelium and preventing its misspecification to a cardiomyogenic fate. *Scf*^{-/-} embryos activated a cardiac transcriptional program in yolk sac endothelium, leading to the emergence of CD31⁺Pdgfr α ⁺ cardiogenic precursors that generated spontaneously beating cardiomyocytes. Ectopic cardiogenesis was also observed in *Scf*^{-/-} hearts, where the disorganized endocardium precociously differentiated into cardiomyocytes. Induction of mosaic deletion of *Scf* in *Scf*^{fl/fl}*Rosa26Cre-ER*^{T2} embryos revealed a cell-intrinsic, temporal requirement for Scf to prevent cardiomyogenesis from endothelium. *Scf*^{-/-} endothelium also upregulated the expression of Wnt antagonists, which promoted rapid cardiomyocyte differentiation of ectopic cardiogenic cells. These results reveal unexpected plasticity in embryonic endothelium such that loss of a single master regulator can induce ectopic cardiomyogenesis from endothelial cells.

INTRODUCTION

The hematopoietic and cardiovascular systems are the first organ systems to develop due to their essential functions in supporting the embryo. Blood cells, the heart, and the vasculature are generated from lateral plate mesoderm (Fehling et al., 2003; Kattman et al., 2006) in a highly coordinated process that ultimately facilitates the circulation of blood cells in the endothelium-lined blood vessels. The high mortality from blood and cardiovascular diseases warrants studies to define the mechanisms that facilitate the establishment and regeneration of these cell types. However, the road map for generating stem/progenitor cells for the different mesodermal lineages is lacking, limiting our ability to derive these cells for clinical use.

It has now been established that the embryonic endothelium not only is a conduit for blood, but also serves as a source of hematopoietic stem/progenitor cells (HS/PCs) (Bertrand et al., 2010; Boisset et al., 2010; Chen et al., 2009; Eilken et al., 2009; Kissa and Herbomel, 2010; Lancrin et al., 2009; Zovein et al., 2008). This unique "hemogenic endothelium" is found during a defined developmental window in intra- and extraembryonic tissues that generate HS/PCs, including the para-aortic splanchnopleura/aorta-gonad-mesonephros (pSP/AGM) region, the yolk sac, and the placenta (Chen et al., 2009; Rhodes et al., 2008; Zovein et al., 2008). However, the mechanisms that govern hemogenic competence in the endothelium are poorly understood.

Fate choice toward cardiovascular and hematopoietic lineages begins when gastrulating cells invaginate through the

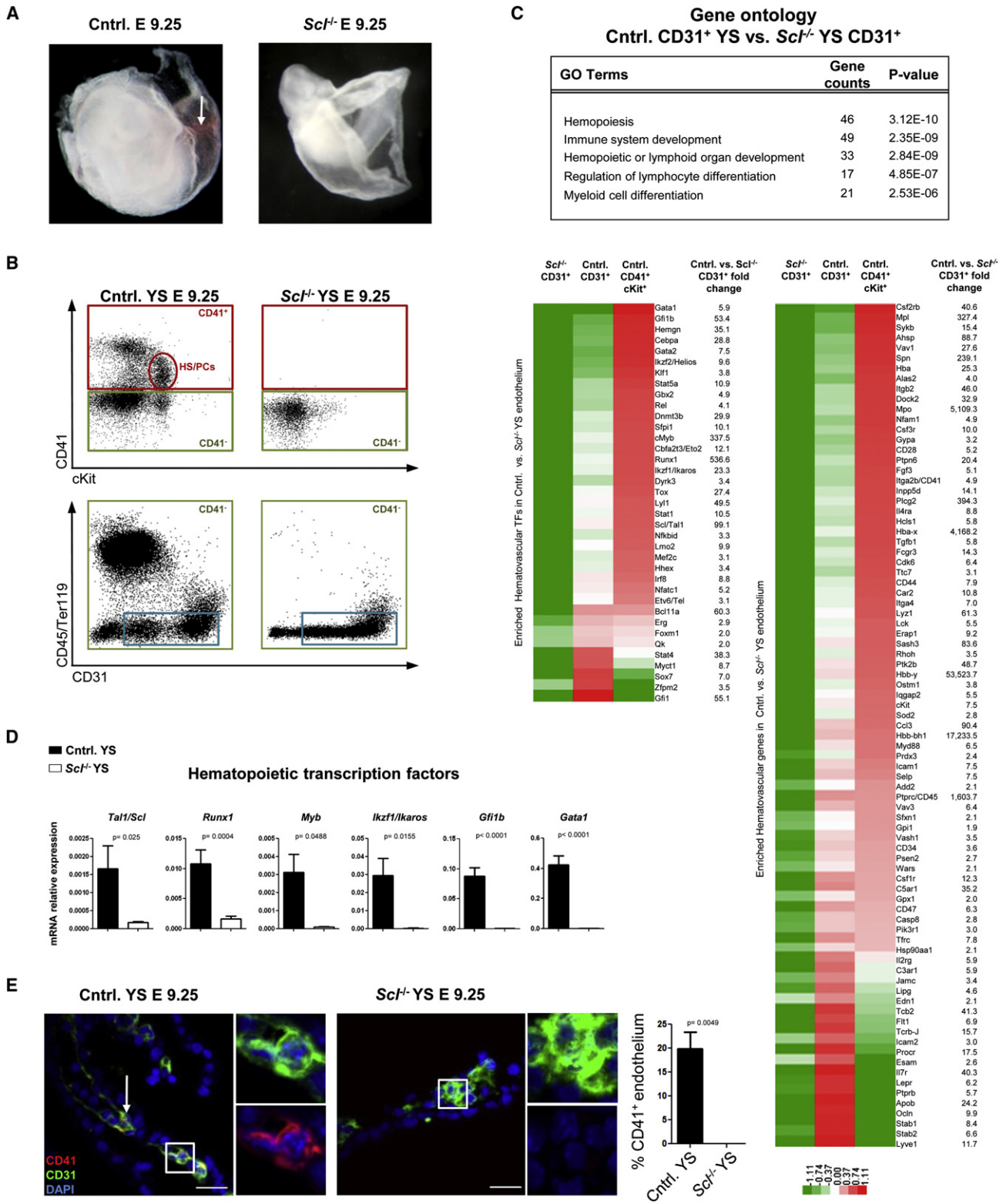


Figure 1. *Scf* Establishes Hemogenic Endothelium in the Yolk Sac

(A) Analysis of E 9.25 *Scf*^{-/-} embryos documented lack of primitive red cells (arrow) and (B) CD41⁺cKit⁺ HS/PCs.

(C) Sorting strategy used to isolate endothelial cells from control and *Scf*^{-/-} yolk sacs (YSs). Cells lacking hematopoietic markers CD41 (green boxes), CD45, and Ter119 but expressing CD31⁺ (blue boxes) were subjected to gene expression analysis.

primitive streak; timing and localization of ingression dictates which morphogens nascent mesodermal cells encounter while migrating to their destination (Kinder et al., 2001). Morphogens that regulate mesodermal fate choice include Wnt, Fgf, TGF β , and BMP (Nostro et al., 2008; Simões et al., 2011). Combinations of these morphogens and their relative levels promote the patterning of the mesoderm to different cardiovascular and hematopoietic fates (Kattman et al., 2006, 2011; Simões et al., 2011).

The bHLH transcription factor Scl/Tal1 is a candidate transcription factor responsible for specifying hemogenic endothelium from mesoderm (Lancrin et al., 2009). *Scf*^{-/-} embryos die by E 9.5 of mouse development due to absence of blood and poorly remodeled vasculature (Shivdasani et al., 1995; Visvader et al., 1998). The requirement for Scl to specify the hematopoietic fate is limited to a narrow window; conditional deletion of Scl using the hematoendothelial-specific *Tie2/Tek Cre* strain or the interferon-inducible *Mx Cre* strain do not disrupt the generation or maintenance of HS/PC pool, although erythropoiesis and megakaryopoiesis are compromised (Mikkola et al., 2003b; Schlaeger et al., 2005). Recent studies revealed that Scl becomes dispensable for HS/PC maintenance due to functional redundancy with a related bHLH factor Lyl1 (Souroullas et al., 2009).

Despite the critical role for Scl in the establishment of the hematopoietic system, little is known about how it generates HS/PCs. Chromatin immunoprecipitation (ChIP)-sequencing in embryonic HS/PCs and erythroid cells revealed widespread binding of Scl and other hematopoietic transcription across thousands of genes, many of which regulate hematopoietic stem cell (HSC) development or maintenance (Kassouf et al., 2010; Wilson et al., 2010). However, these genome-wide binding studies have provided little information about the genes that depend on each of these factors for their expression.

Here we show that Scl establishes hemogenic endothelium by activating transcription factors required for HS/PC emergence and self-renewal. Moreover, our studies revealed an unexpected repressive role for Scl, as loss of Scl resulted in the generation of ectopic cardiomyocytes in yolk sac vasculature and the endocardium. These results uncover remarkable developmental plasticity in embryonic vasculature and identify Scl as a key determinant of endothelial fate choice.

RESULTS

Scl Establishes Hemogenic Competence in Endothelium

Embryos devoid of Scl lack embryonic red cells and HS/PCs in all hematopoietic tissues (Figures 1A and 1B; Figure S1A available online), providing an ideal in vivo model to study the establishment of the hematopoietic system. To determine which

hematopoietic genes are activated in the endothelium in the yolk sac by Scl, we performed microarray analysis on *Scf*^{-/-} and control CD31⁺ cells that were depleted of hematopoietic cells and compared them to CD41⁺cKit⁺ HS/PCs from control yolk sacs. Gene ontology enrichment analysis of the 1,295 differentially expressed genes (Table S1a) downregulated in *Scf*^{-/-} endothelium (>1.5-fold, *p* < 0.05) revealed a robust Scl-dependent hematopoietic transcriptional program in yolk sac endothelium. These genes included transcription factors regulating HSC development (*Runx1*, *cMyb*, *Fli1*), self-renewal (*Etv6/Tel*, *Izkf1/Ikaros*, *Erg*, *Gfi1*), and differentiation (*Gata1* and *Gfi1b*), as well as surface proteins expressed on hematopoietic cells (*Itga2b/CD41*, a marker of nascent HS/PCs (Bertrand et al., 2005; Mikkola et al., 2003a) and the panhematopoietic marker *Ptprc/CD45*) (Figure 1C). Quantitative PCR (qPCR) on yolk sacs verified Scl dependence of key hematopoietic transcription factors (Figure 1D). Immunofluorescence (IF) validated robust coexpression of CD41 in CD31⁺ endothelium of control but not *Scf*^{-/-} yolk sacs (Figure 1E). These data indicate that Scl activates a network of hematopoietic transcription factors necessary for hemogenic competence in the endothelium.

Loss of Scl Provokes Ectopic Cardiogenesis in Hemogenic Tissues

To evaluate whether Scl has a repressive function in the endothelium in hemogenic tissues, GO enrichment analysis was performed for the 965 genes upregulated in CD31⁺ cells in *Scf*^{-/-} yolk sacs. Unexpectedly, several highly significant GO categories were related to cardiogenesis and heart function (Figure 2A). The upregulated genes included key cardiac transcription factors such as *Isl1*, *Myocd*, *Smarcd3*, and *Tbx5*, as well as several cardiomyocyte-specific structural proteins including *Tnnt2*, *Myl7*, *Actc1*, *Myh6*, *Myh7*, and *Ryr2* (Figure 2A; Table S1b). qPCR analysis confirmed ectopic expression of cardiac genes in *Scf*^{-/-} yolk sacs (Figure 2B), while fluorescence-activated cell sorting (FACS) documented a population of cells expressing Troponin T (data not shown). IF revealed frequent coexpression of Troponin I (9.0 ± 4.5%) or T (19.5 ± 0.5%) in CD31⁺ cells in *Scf*^{-/-} yolk sacs (Figure 2C), and whole mount staining identified clusters of ectopic cardiomyocytes scattered throughout the yolk sac (Figure 2D). Furthermore, explant cultures of *Scf*^{-/-} yolk sacs produced colonies of synchronously beating cardiomyocytes (Movies S1A and S1B; Figure 2E). Formation of beating colonies from *Scf*^{-/-} yolk sacs was highly reproducible (26/28), and, in some cases, individual beating cells were observed after as few as 4 hr in culture, indicating that ectopic cardiomyocytes had matured in situ (Movie S1C). Cardiomyocytes from *Scf*^{-/-} yolk sacs evidenced spontaneous calcium transients, which could be inhibited by the calcium channel blocker nifedipine. Moreover, ectopic cardiomyocytes

(C) Heat maps represent the relative expression and fold change of hematopoietic transcription factors (TFs) and other proteins significantly downregulated (>1.5-fold, *p* < 0.05) in *Scf*^{-/-} versus control YS endothelium; expression in control CD41⁺cKit⁺ HS/PCs is shown for comparison. Selected GO categories derived from differentially expressed genes are listed.

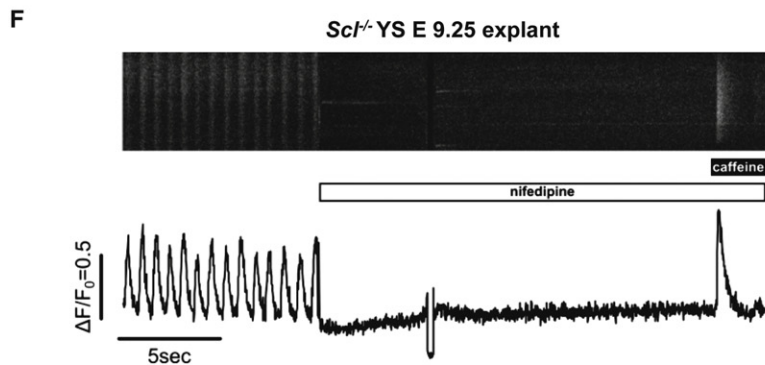
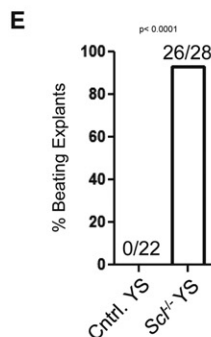
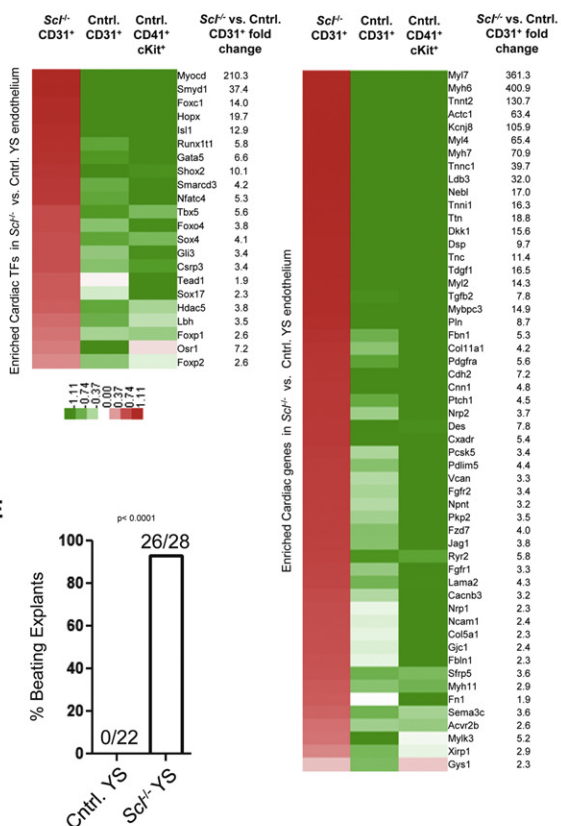
(D) qPCR for hematopoietic TFs on E 9.25 unfractionated YSs; mean of four biological replicates normalized to *HPRT* is shown.

(E) IF for Scl-dependent HS/PC marker CD41 (*n* = 3); insets are higher magnification, single channel + DAPI images of boxed areas. Scale bar, 25 μ m. In all panels, error bars represent SEM.

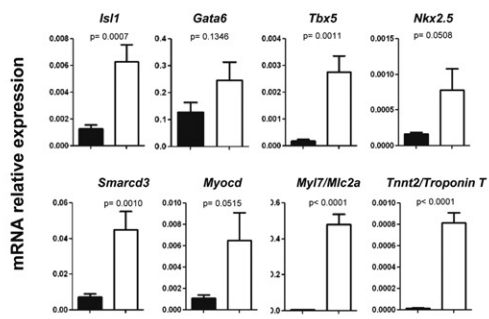
See also Figure S1 and Tables S1A and S2A.

A Gene ontology
Scf^{-/-} YS CD31⁺ vs. Cntrl. YS CD31⁺

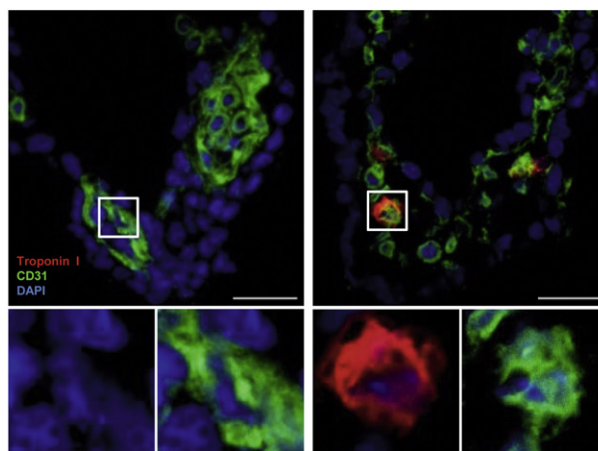
GO Terms	Gene counts	P-value
Heart development	42	8.67E-16
Cell adhesion	69	2.02E-15
Muscle organ development	31	5.25E-11
Cardiac muscle tissue development	18	9.67E-11
Extracellular matrix organization	21	6.23E-09



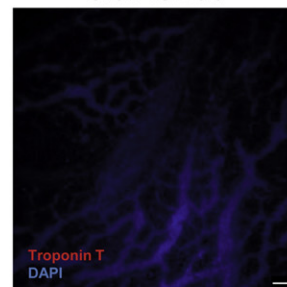
B ■ Cntrl. YS ■ *Scf*^{-/-} YS
Cardiac transcription factors and structural proteins



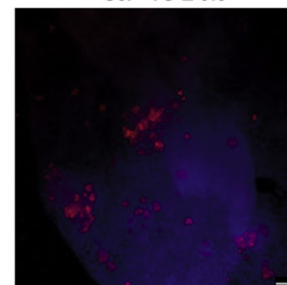
C Cntrl. YS E 9.25 *Scf*^{-/-} YS E 9.25



D Cntrl. YS E 9.5



Scf^{-/-} YS E 9.5



were capable of storing Ca^{2+} within the sarcoplasmic reticulum, which was susceptible to caffeine-induced release (Figure 2F). These results demonstrate that *Scl* is critical for suppressing cardiomyogenesis in the yolk sac.

Scl Activates Hematopoiesis and Represses Cardiogenesis in Placental Vasculature

To investigate if *Scl* also modulates endothelial fate in other hematopoietic tissues, we performed microarray analysis on CD31^+ cells in the placenta, another site that can generate multipotent HS/PCs (Rhodes et al., 2008; Zeigler et al., 2006). These results verified that also in placental endothelium, *Scl* activates many of the same hematovascular transcription factors as in the yolk sac, with the addition of *Sox17* and *Bmi1* that regulate self-renewal of fetal and adult HSCs (Kim et al., 2007; Park et al., 2003) (Table S2a). No significant expression of cardiac structural proteins was detected in *Scl*^{-/-} placental endothelium; however, there was expression of transcription factors essential for cardiac progenitor cell function including *Isl1* and *Smyd1*, as well as cardiac morphogenesis genes including *Has2*, *Dkk1*, and *Vcan* (Figures S1B and S1C; Table S2b). These results indicate that the misspecification of prospective hemogenic endothelium to the cardiac fate is not limited to the yolk sac.

Loss of Scl Leads to the Emergence of CD31⁺Pdgfra⁺ Cardiogenic Cells from Prospective Hemogenic Endothelium

To identify the cardiogenic cells in the vasculature, we screened the microarray data for surface proteins upregulated in *Scl*^{-/-} endothelium in both the yolk sac and the placenta. *Pdgfra*, a marker of cardiogenic mesoderm (Kattman et al., 2011), was significantly upregulated in *Scl*^{-/-} endothelium in both tissues (Figure 2A; Figure S1C). FACS analysis of E 9.25 conceptuses identified a subpopulation of CD31^+ cells coexpressing *Pdgfra* in all hematopoietic tissues in *Scl*^{-/-} embryos (Figure 3A). By E 8.5, $\text{CD31}^+\text{Pdgfra}^+$ cells had already formed in the *Scl*^{-/-} yolk sac but were just emerging in the placenta (Figure S2A). $\text{CD31}^+\text{Pdgfra}^+$ cells were not found in hematopoietic tissues in controls (Figure 3A), even at an earlier developmental stage (Figure S2A).

Microarray analysis comparing $\text{CD31}^+\text{Pdgfra}^-$ endothelial cells and $\text{CD31}^+\text{Pdgfra}^+$ putative cardiogenic cells from *Scl*^{-/-} yolk sacs revealed upregulation of cardiac transcription factors and structural proteins in $\text{CD31}^+\text{Pdgfra}^+$ cells (Figure 3B;

Table S3a), while the expression of many vascular genes (*Kdr*, *Flk1*, *Esam1*, *Cdh5*/*Ve-cadherin*, etc.) was downregulated (Table S3b; Figures S2B and S2C). qPCR for *Isl1* and *Gata6* on sorted cells from the yolk sac and the placenta confirmed the upregulation of cardiac transcription factors in $\text{CD31}^+\text{Pdgfra}^+$ cells (Figure 3C). The head endothelium in *Scl*^{-/-} embryos neither generated $\text{CD31}^+\text{Pdgfra}^+$ cells (Figure 3A) nor expressed cardiac transcription factors (Figure 3C). These data verify cardiac identity of $\text{CD31}^+\text{Pdgfra}^+$ cells and suggest that the ectopic cardiogenesis in *Scl*^{-/-} embryos is restricted to a specific type of endothelium.

Of note, comparison of gene expression in $\text{CD31}^+\text{Pdgfra}^-$ endothelial cells between *Scl*^{-/-} and control yolk sacs revealed that the cardiogenic transcriptional program was initiated in endothelial cells (Figure S2D; Table S3c). Furthermore, IF for CD31 and *Pdgfra*⁺ in *Scl*^{-/-} yolk sacs documented integration of $\text{CD31}^+\text{Pdgfra}^+$ cardiogenic cells within the vasculature (Figure 3D). To functionally assess the developmental potential of $\text{CD31}^+\text{Pdgfra}^-$ endothelium and $\text{CD31}^+\text{Pdgfra}^+$ cells in *Scl*^{-/-} embryos, we sorted these populations and plated them in cardiac differentiation conditions. Both populations from *Scl*^{-/-} yolk sac had the potential to generate cardiomyocytes, as evidenced by Troponin T expression, presence of organized sarcomeres, and spontaneous beating (Figures 3E and S2E; Movies S2A, S2B, S2C). Altogether, these data indicate that, in the absence of *Scl*, endothelium in the yolk sac becomes misspecified to cardiac fate.

The Requirement for Scl to Repress Cardiogenesis in Hemogenic Tissues Is Cell Autonomous and Temporally Defined

As the misspecified endothelium expressed both cell-intrinsic (e.g., transcription factors) and secreted factors (e.g., Wnt inhibitors *Dkk1*, *Sfrp1*, *Sfrp5*, and *Frzb*) that promote cardiac differentiation, we asked if *Scl* acts cell autonomously to prevent cardiogenesis in hematopoietic tissues and crossed tamoxifen-inducible *Rosa26Cre-ER^{T2}* mice with *Scl^{fl/fl}* mice (Figure 4A). Injection of tamoxifen results in a peak of the active drug 12 hr later, which facilitates nuclear localization of Cre (Zovein et al., 2008). Injection of tamoxifen at E 6.5 did not result in a significant difference in the hematopoietic compartment; however, $\text{CD31}^+\text{Pdgfra}^+$ cardiogenic cells appeared in a majority of *Rosa26-Cre-ER^{T2}Scl^{fl/fl}* yolk sacs (Figure 4B) and placentas (data not shown). Coexistence of hematopoiesis and ectopic cardiomyogenesis in *Rosa26Cre-ER^{T2}Scl^{fl/fl}* yolk sacs was verified by

Figure 2. Lack of Scl Induces Cardiomyogenesis in YS Vasculature

(A) Selected GO categories encompassing genes upregulated in *Scl*^{-/-} YS endothelium are shown. Heat maps represent the relative expression and fold change of known cardiac TFs and other proteins significantly upregulated (>1.5-fold, $p < 0.05$) in *Scl*^{-/-} versus control YS CD31^+ cells. $\text{CD41}^+\text{cKit}^+$ HS/PCs are shown for comparison.

(B) qPCR for cardiac TFs and cardiomyocyte structural genes on E 9.25 unfractionated YSs; mean of four biological replicates normalized to *HPRT* is shown.

(C) IF for Troponin I ($n = 2$; Troponin T, $n = 3$) and CD31 on YS sections; insets are higher magnification, single channel + DAPI images of boxed areas. Scale bar, 25 μm .

(D) Whole mount IF for Troponin T on YSs. Scale bar, 50 μm .

(E) Frequency of YSs generating beating colonies in explant culture (see Movie S1).

(F) *Scl*^{-/-} YS explants were loaded with Fluo4-AM and spontaneous calcium transients were measured using confocal microscopy. Nifedipine (10 μM) and caffeine (10 mM) were added at the indicated times. In all panels, error bars represent SEM.

See also Figure S1, Tables S1B and S2B, and Movie S1.

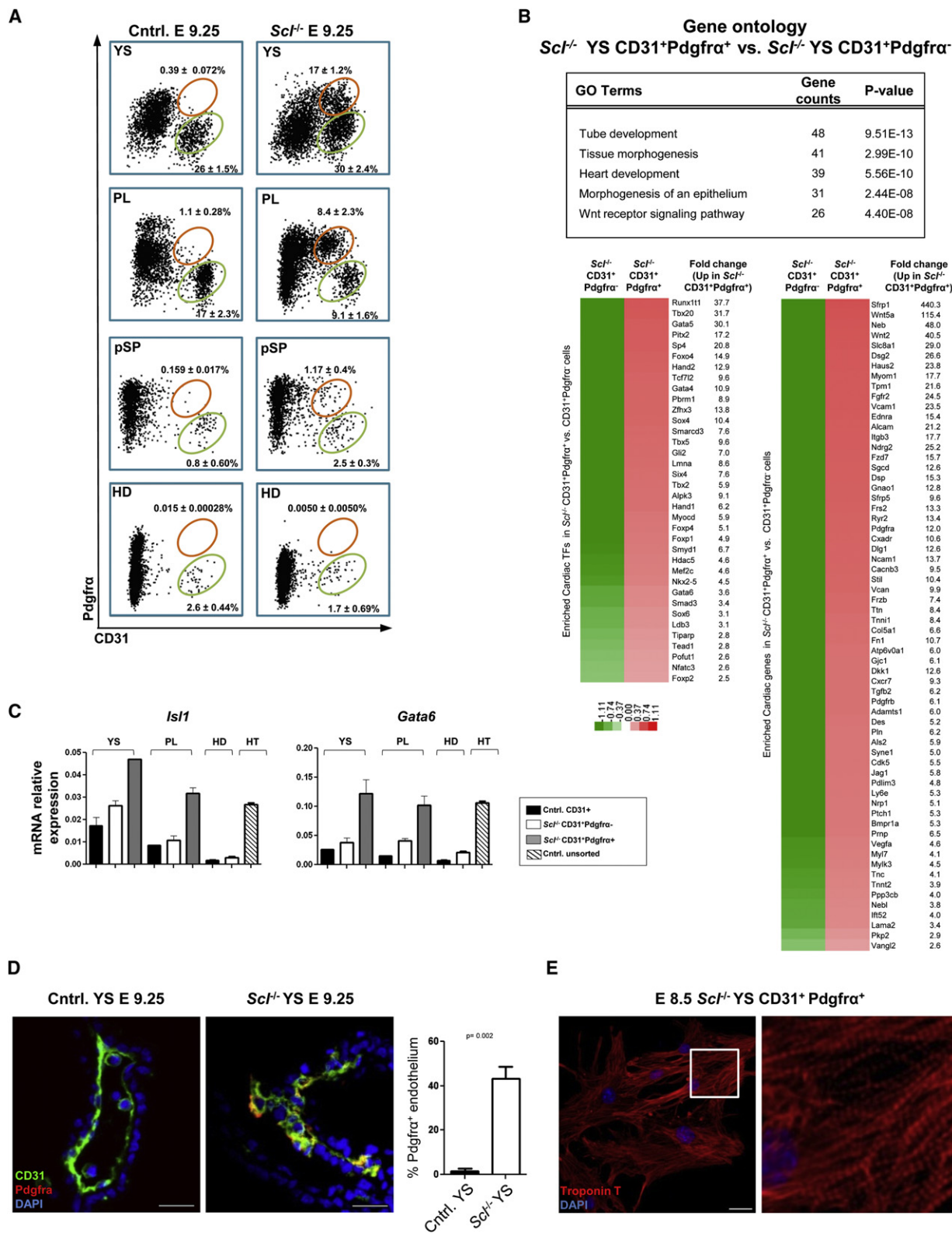


Figure 3. *Scf* Represses the Development of CD31⁺Pdgfra⁺ Cardiac Cells in Hemogenic Tissues

(A) FACS on cells depleted for CD41, CD45, and Ter119 showing CD31⁺Pdgfra⁺ cells (orange gates) and CD31⁺ endothelial cells (green gates) in embryonic tissues (PL, placenta; pSP, para-aortic splanchnopleura; HD, head). Mean ± SEM of at least three biological replicates is shown.

qPCR (Figure 4C). Although the deletion at the *Scf* locus in *Rosa26Cre-ER^{T2}Scf^{fl/fl}* yolk sacs was only partial, PCR for sorted CD31⁺Pdgfra⁺ cardiogenic cells demonstrated full excision of both targeted alleles (Figure 4D). These data verify a cell-intrinsic requirement for *Scf* in repressing ectopic cardiogenesis.

To investigate whether the requirement for *Scf* to repress the cardiomyogenesis continues after mesodermal fates have diverged, we initiated injection at E 7.5 and the embryos were harvested at E 10.5. In spite of later deletion, many *Rosa26-Cre-ER^{T2}Scf^{fl/fl}* yolk sacs still generated CD31⁺Pdgfra⁺ cells (Figure 4E) and expressed cardiac transcription factors and structural proteins (Figure 4F). CD31⁺Pdgfra⁺ cells were also observed in 2/8 placentas (data not shown). However, when the deletion was induced a day later, at E 8.5, cardiac conversion was no longer observed despite comparable excision efficiency (Figures 4G and 4H; data not shown). These data suggest that *Scf* is required for the repression of the cardiac fate in hemogenic tissues for a limited developmental window.

Scf Inhibits Cardiomyocyte Differentiation in the Endocardium

As the loss of *Scf* induced ectopic cardiogenesis from endothelium in hematopoietic tissues, we next examined *Scf^{-/-}* hearts for evidence of endothelial misspecification. The heartbeat was initiated in *Scf^{-/-}* hearts despite structural defects and pericardial effusion (Figure 5A; data not shown). *Scf^{-/-}* outflow tracts and right ventricles were hypomorphic compared to the left ventricle, and the atrial and ventricular septa were poorly formed. Moreover, the heart chambers were filled with poorly organized endocardium (Figures 5A and 5B). IF for CD31 and Troponin T revealed that a substantial population (16.7 ± 3.8%) of endocardial cells coexpressed cardiomyocyte-specific proteins (Figure 5B), demonstrating misspecification of *Scf^{-/-}* endocardium to cardiomyocytic fate.

Notably, CD31⁺Pdgfra⁺ cells were found in both *Scf^{-/-}* and control hearts, although they emerged earlier (E 8.5) and were more frequent (E 9.25) in *Scf^{-/-}* hearts (Figure 5C). Microarray analysis of CD31⁺Pdgfra⁻ and CD31⁺Pdgfra⁺ cells from control and *Scf^{-/-}* hearts revealed upregulation of the cardiomyogenic transcriptional program in both *Scf^{-/-}* endocardium and CD31⁺Pdgfra⁺ cells (Figures 5D and 5E; Table S4). In functional assays, both the endocardium and CD31⁺Pdgfra⁺ cells from *Scf^{-/-}* hearts generated beating cardiomyocytes that expressed Troponin T and displayed organized sarcomeres (Movies S3A, S3B, and S3C; Figure 5F). These data indicate that *Scf* suppresses cardiomyocyte differentiation of endocardium and CD31⁺Pdgfra⁺ cells in the heart.

The Requirement for Scf to Suppress Cardiomyocyte Fate Extends Perinatally in the Heart

We next assessed whether the timing when *Scf* is required to suppress cardiomyocyte differentiation in the heart correlates with that in hemogenic tissues (Figure S3A). When induction was initiated at E 6.5 and embryos harvested at E 9.5, the expression of cardiac structural proteins (e.g., *Myl7*) was significantly increased in both CD31⁺Pdgfra⁻ endocardial cells and CD31⁺Pdgfra⁺ cells in *Rosa26Cre-ER^{T2}Scf^{fl/fl}* embryos (Figure S3B). Upregulation of *Myl7* was also observed in CD31⁺Pdgfra⁺ cells in *Rosa26Cre-ER^{T2}Scf^{fl/fl}* hearts upon later induction at E 8.5 or 16.5 (harvest at E 11.5 and 19.5, respectively), after cardiogenic potential in the yolk sac had subsided (Figures S3C and S3D). Remarkably, in some cases, sorted CD31⁺Pdgfra⁺ cells from *Rosa26Cre-ER^{T2}Scf^{fl/fl}* perinatal hearts (E 19.5) generated spontaneously beating Troponin T⁺ cardiomyocytes (Figure S3D and Movie S4). These data indicate that the requirement for *Scf* to repress the cardiomyocyte fate continues perinatally in CD31⁺Pdgfra⁺ cells in the heart (Figure S3E).

CD31⁺Pdgfra⁺ Putative Cushion Mesenchymal Cells Emerge from *Ve-cadherin⁺Isl1⁺* Precursors during Normal Development

As the requirement to repress cardiomyocyte differentiation in the later heart became confined to CD31⁺Pdgfra⁺ cells, we sought to define their identity and origin. CD31⁺Pdgfra⁺ cells in control hearts appeared first by E 9.25; their frequency peaked at around E 10.5 and then declined, although a small population persisted until early postnatal life (Figure S4A). IF demonstrated that CD31⁺Pdgfra⁺ cells in control hearts at E 9.5 were localized specifically to the outflow tract (OFT) and the atrioventricular canal (AVC) (Figure S4B), in contrast to *Scf^{-/-}* hearts where CD31⁺Pdgfra⁺ cells were found throughout the heart (data not shown). Microarray analysis showed that the CD31⁺Pdgfra⁺ cells in normal hearts were enriched for cardiac transcription factors *Smarcd3*, *Hand1*, *Gata4*, and *Gata6* (Figure S4C; Tables S4e and S4f) and expressed several transcription factors associated with EMT (epithelial-mesenchymal transition) including *Twist1*, *Snai1*, *Twist2*, and *Zeb2*. Furthermore, several genes involved in endocardial cushion morphogenesis, including *Erbb3*, *Sox9*, *Msx1*, *Tgfb2*, and *Vcan*, were upregulated in CD31⁺Pdgfra⁺ cells. Based on the timing when CD31⁺Pdgfra⁺ cells were found in normal hearts, their localization in the OFT and AVC, and gene expression, we concluded that this population contains precursors of cardiac cushion mesenchymal cells.

We next investigated whether the CD31⁺Pdgfra⁺ cells in the heart have similar lineage relationship with endothelial cells as HS/PCs in hemogenic tissues and performed lineage tracing using the endothelial *Ve-cadherin Cre* strain bred to the

(B) Gene expression analysis of CD31⁺Pdgfra⁻/CD31⁺Pdgfra⁺ cells from *Scf^{-/-}* YSs. Differentially expressed (>1.5-fold, *p* < 0.05) cardiac TFs, and other proteins enriched in CD31⁺Pdgfra⁺ cells with their fold changes, as well as selected GO categories, are shown.

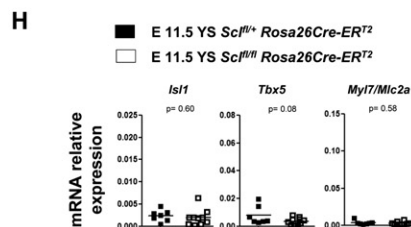
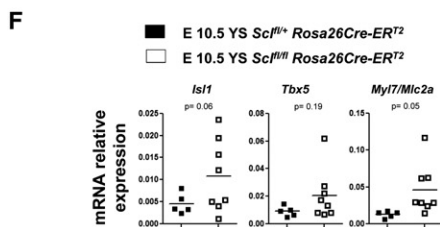
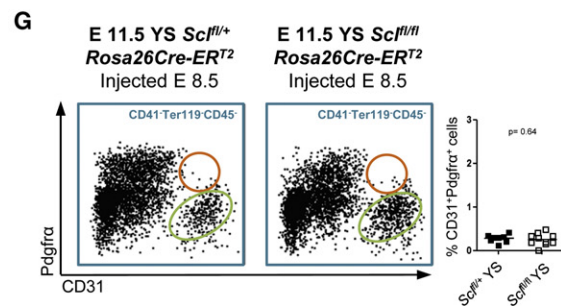
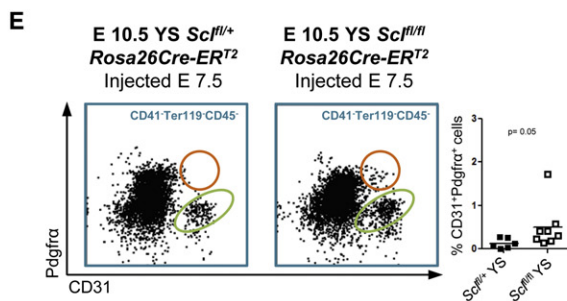
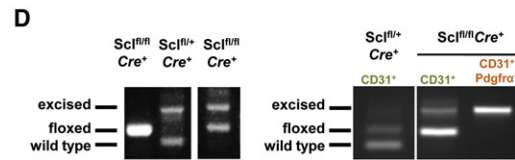
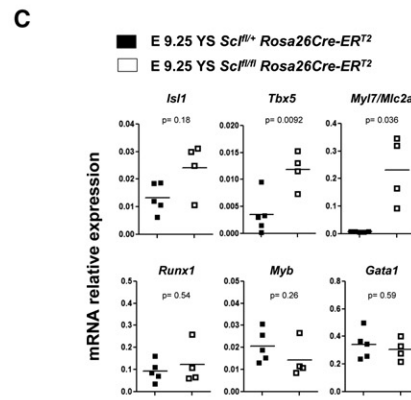
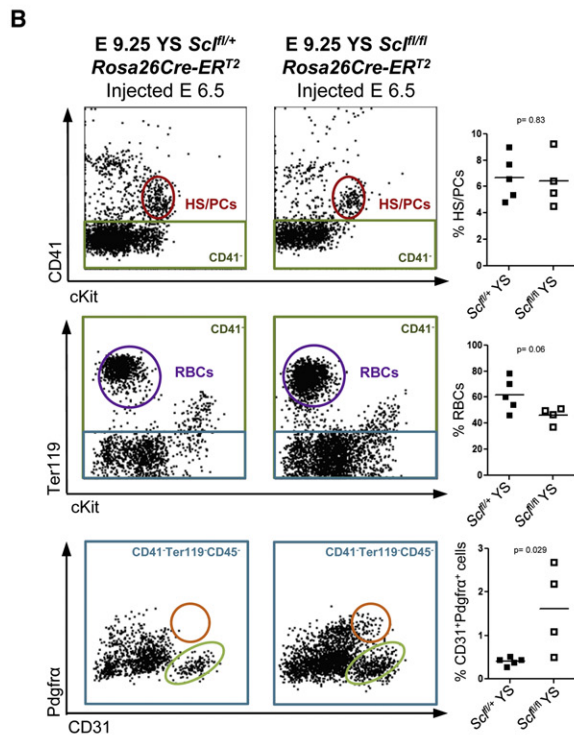
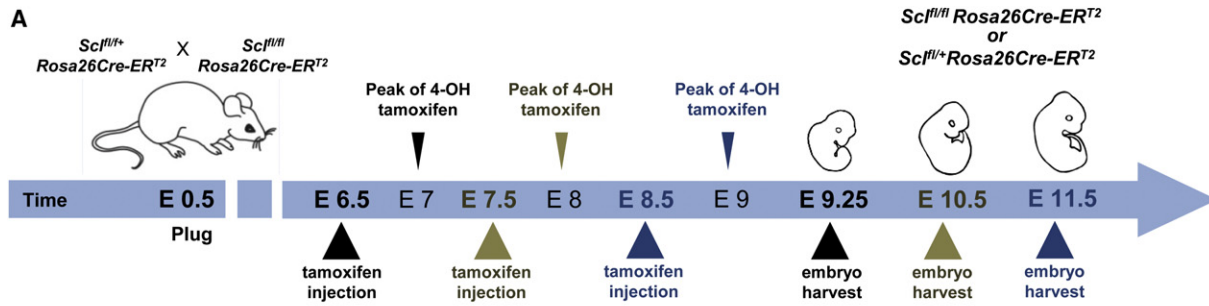
(C) qPCR for cardiac TFs on indicated populations sorted from YS, PL, and HD; unfractionated heart (HT) was used as a positive control. Mean ± SD of technical replicates from pooled samples normalized to actin is shown.

(D) IF for CD31 and Pdgfra on YS sections (*n* = 3; mean ± SEM is shown). Scale bar, 25 μm.

See Movie S2.

(E) CD31⁺Pdgfra⁺ cells were sorted from E 8.5 *Scf^{-/-}* YSs, cultured and stained for Troponin T. Scale bar, 25 μm.

See also Figure S2, Table S3, and Movie S2.



Rosa26-YFP reporter strain (Figure S4D) (Alva et al., 2006; Stadtfeld and Graf, 2005). In the heart, both CD31⁺Pdgfra⁻ endothelial cells as well as CD31⁺Pdgfra⁺ cushion mesenchymal cells evidenced equally efficient marking by the *Ve-cadherin Cre* (Figure S4D), although the latter had downregulated endothelial genes (Figure S4E). The efficiency of lineage tracing in placental and yolk sac endothelium and circulating HS/PCs was similar to that observed in the heart (data not shown). These results further strengthen the hypothesis that CD31⁺Pdgfra⁺ cells represent cushion mesenchymal cells, which are derived from endocardium (de Lange et al., 2004). Furthermore, lineage tracing using *Isl1 Cre* (Cai et al., 2003)—a transcription factor regulating multipotent cardiac progenitors (Moretti et al., 2006)—revealed that a large fraction of the endocardium and CD31⁺Pdgfra⁺ cells originate from *Isl1*⁺ precursors (Figure S4F). Moreover, analysis of *Isl1*^{-/-} hearts revealed that the establishment of CD31⁺Pdgfra⁺ cells was *Isl1* dependent (Figure S4G). These data suggest that CD31⁺Pdgfra⁺ cells in the wild-type heart represent cushion mesenchymal cells and are distinct from the ectopic cardiomyogenic CD31⁺Pdgfra⁺ cells in *Scf*^{-/-} hearts.

Runx1 and Isl1 Do Not Have a Critical Effect on Cardiac Misspecification of Endothelium

To understand the mechanisms downstream of *Scf* that modulate hematopoietic versus cardiac development in the endothelium, we asked if the emergence of CD41⁺cKit⁺ HS/PCs or CD31⁺Pdgfra⁺ cardiogenic cells was dependent on known HS/PC or cardiac progenitor transcription factors that *Scf* regulates. Analysis of *Runx1*^{-/-} embryos verified that the emergence of HS/PCs from hemogenic endothelium was *Runx1* dependent (Figure 6A). However, in contrast to *Scf*^{-/-} embryos, no CD31⁺Pdgfra⁺ cells were detected in hematopoietic tissues in *Runx1*^{-/-} embryos, nor was this population expanded in the heart (Figures 6B and 6C). Lack of ectopic cardiac differentiation in *Runx1*^{-/-} yolk sacs was further confirmed by qPCR (Figure 6E). These results imply that, despite its pivotal role in the transition of hemogenic endothelium to HS/PCs, *Runx1* is not required to repress cardiac conversion of endothelium (Figure 6F).

As *Isl1*^{-/-} embryos showed a drastic reduction of CD31⁺Pdgfra⁺ cells in the heart (Figure S4G), we asked whether generation of cardiogenic CD31⁺Pdgfra⁺ cells in *Scf*^{-/-} embryos was also dependent on *Isl1* and generated *Scf*^{-/-}*Isl1*^{-/-} embryos. Morphologically, *Scf*^{-/-}*Isl1*^{-/-} embryos evidenced a compound phenotype with absence of blood, smaller embryonic size, and lack of pharyngeal arches and cardiac outflow tract (Figure 6D). It is interesting that CD31⁺Pdgfra⁺ cells were generated in the yolk sac and the heart of *Scf*^{-/-}*Isl1*^{-/-} embryos, and cardiac transcription factors and structural proteins, including *Gata6*, *Smarcd3*, *Myocd*, *Tnnt2*, and *Myl7*, were ectopically expressed

(Figure 6E). These data indicate that cardiac conversion in *Scf*^{-/-} endothelium is independent of *Isl1* (Figure 6F).

Cardiomyocyte Differentiation from Endothelium Is Promoted by Wnt Antagonism

We next sought to define the mechanisms that promote the rapid cardiomyocyte differentiation in the endothelium of *Scf*^{-/-} yolk sacs and hearts. Notably, expression of cardiac transcription factors *Isl1* and *Tbx5*, as well as structural proteins *Myl7* and *Tnnt2*, were induced in *Scf*^{-/-} yolk sacs by E 8.5, concurrent with the appearance of CD31⁺Pdgfra⁺ cells (Figures 7A and S2A). Likewise, expression of several canonical Wnt antagonists including *Dkk1*, *Frzb*, *Sfrp1*, and *Sfrp5* that promote terminal cardiomyocyte differentiation (David et al., 2008; Jaspard et al., 2000; Schneider and Mercola, 2001) was also observed at E 8.5 (Figure 7B). We therefore asked whether *Scf*^{-/-} endothelial cells respond to Wnt inhibition. Indeed, gene set enrichment analysis (GSEA) comparing *Scf*^{-/-} yolk sacs with expression data from differentiating mouse embryoid bodies treated with the Wnt inhibitor *Dkk1* (Lindsley et al., 2008) revealed a highly significant correlation of gene expression, indicating that *Scf*^{-/-} endothelial cells are responding to canonical Wnt inhibition (Figure 7C). Similar correlations were also observed in the heart and the placenta (Figures S5A and S5B).

As Wnt inhibitors are known to promote differentiation of cardiac cells, we asked if the ectopic cardiogenic cells in *Scf*^{-/-} tissues respond to Wnt agonists to preserve a more undifferentiated state. Pregnant dams carrying *Rosa26Cre-ER^{T2}Scf^{fl/fl}* embryos were first injected with tamoxifen at E 6.5 to induce cardiogenic conversion and subsequently stimulated by the Wnt agonist LiCl, or control NaCl, after which yolk sacs were assayed for cardiomyocyte gene expression at E 11.5. qPCR revealed that the expression of cardiac structural proteins *Myl7* and *Tnnt2* was significantly reduced upon Wnt stimulation (Figure 7D). Moreover, when *Scf*^{-/-} yolk sacs were plated in explant culture and supplemented either with LiCl or NaCl throughout the 9 to 10-day culture, the colonies containing beating cardiomyocytes were larger and their size continued to increase over several days upon Wnt stimulation (Figure 7E). These results indicate that, in vivo, *Scf*^{-/-} ectopic cardiogenic precursors experience Wnt antagonism that promotes cardiomyocyte differentiation; however, at least a subset of these cells retain the capacity to respond to Wnt stimulation (Figure 7F).

DISCUSSION

Our work has uncovered unexpected cardiogenic potential in prospective hemogenic endothelium in blood-forming tissues and endocardium in the heart. Upon loss of a single transcription

Figure 4. *Scf* Has a Cell-Autonomous, Temporally Defined Role in Preventing Ectopic Cardiogenesis in Hemogenic Tissues

(A) Tamoxifen-inducible *Rosa26Cre-ER^{T2}* mouse strain was used to delete *Scf* at desired time points.

(B, E, and G) FACS for CD41⁺cKit⁺ HS/PCs (red ovals) and Ter119⁺ RBCs (purple circles) in *Rosa26Cre-ER^{T2}Scf^{fl/fl}* and *Rosa26Cre-ER^{T2}Scf^{fl/fl}* YSs of pregnant dams injected at E 6.5 (B), E 7.5 (E), and F 8.5 (G). Analysis for CD31⁺ cells (green ovals) and CD31⁺Pdgfra⁺ cells (orange circles) is shown. Graphs show frequencies of HS/PCs, RBCs, and CD31⁺Pdgfra⁺ cells in individual embryos.

(C, F, and H) qPCR for cardiac and/or hematopoietic genes on YSs following injection at E 6.5 (C), E 7.5 (F), and (H) E 8.5. Graphs show mRNA expression level normalized to *HPRT* in individual embryos. (D) PCR of embryonic head DNA (left) isolated from embryos injected at E 6.5 and harvested at E 9.5. PCR from CD31⁺Pdgfra⁻ versus CD31⁺Pdgfra⁺ cells sorted from *Rosa26Cre-ER^{T2}Scf^{fl/fl}* YSs (right).

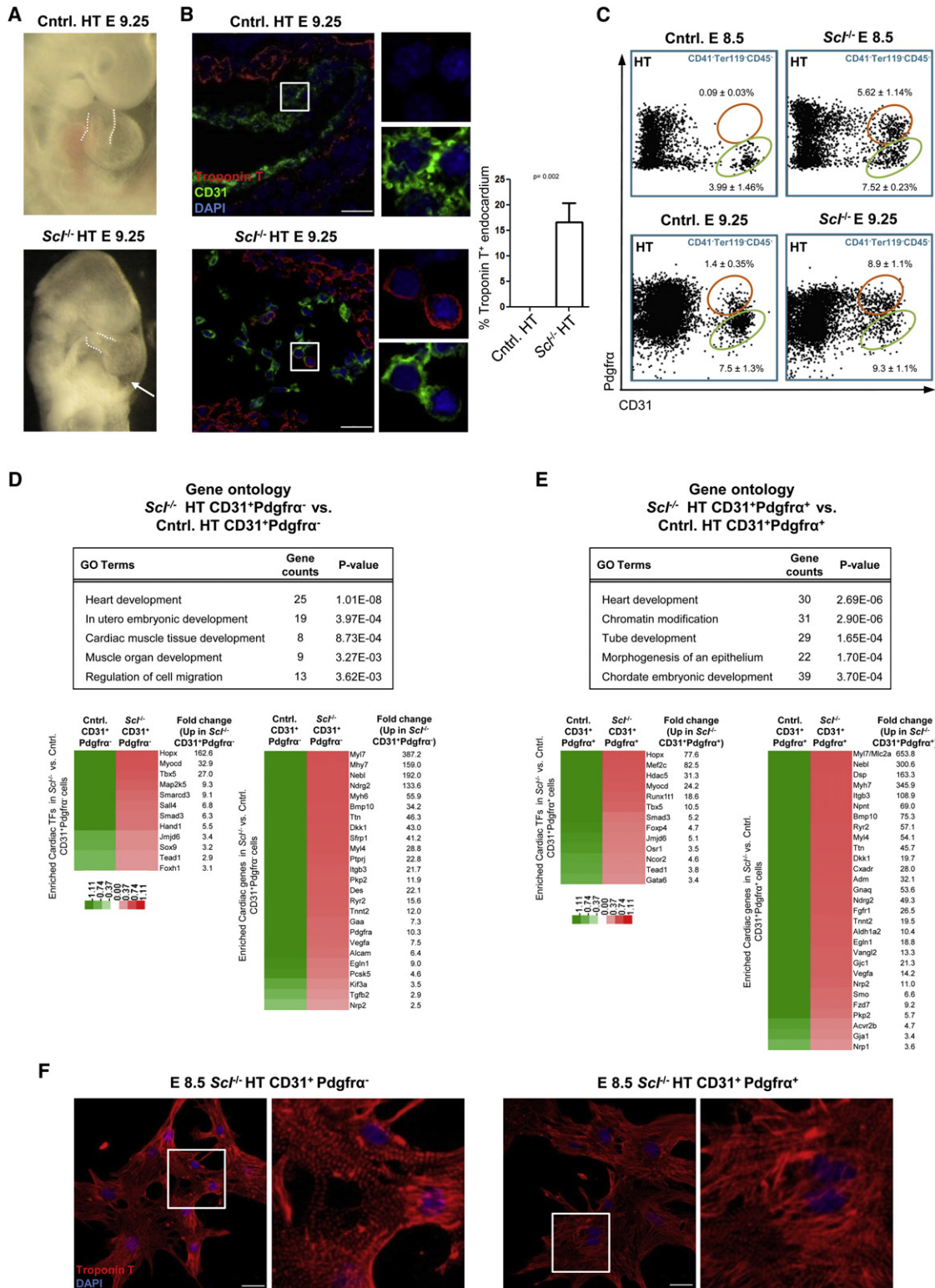


Figure 5. *Scf*^{-/-} Endocardium Is Misspecified to Cardiomyogenic Fate

(A) *Scf*^{-/-} hearts evidenced malformed outflow tract (dotted lines) and pericardial effusion (arrow).

(B) IF for CD31 and Troponin T on heart sections (n = 3; mean ± SEM is shown). Scale bar, 25 μm.

(C) FACS for CD31⁺ endocardial cells (green ovals) and CD31⁺Pdgfra⁺ cells (orange circles) in the heart at E 8.5 and E 9.25. Mean ± SEM of at least three biological replicates is shown.

factor, *Scl*, endothelium in these tissues gives rise to cardiogenic precursors that differentiate into spontaneously beating cardiomyocytes. The temporal window when *Scl* is required to repress cardiomyogenesis in hematopoietic tissues closely parallels the timing of HS/PC specification in hemogenic endothelium, while in the heart, the repressive function of *Scl* continues perinatally in CD31⁺Pdgfra⁺ putative cushion mesenchymal cells. Previous studies had suggested that *Scl* has mesoderm patterning activity during early development, as overexpression of *Scl* in mesoderm during embryonic stem cell differentiation promoted hematopoiesis at the expense of cardiac and paraxial mesoderm (Ismailoglu et al., 2008). Likewise, modulation of *Scl* and *Etsrp* (zebrafish homolog for *Etv2/ER71*) expression altered the size of the heart field (Schoenebeck et al., 2007), and loss of *Etsrp/Etv2* induced cardiomyocyte gene expression in endocardial progenitors (Palencia-Desai et al., 2011; Rasmussen et al., 2011). These studies delineate a critical function for *Scl* and its upstream regulator *Etsrp/Etv2* in promoting hematovascular fates over cardiac potential during mesoderm specification. Nevertheless, our finding that loss of *Scl* in the endothelium in hemogenic tissues and the heart after mesodermal tissues have diverged can give rise to fully functional, beating cardiomyocytes reveals unforeseen developmental plasticity in embryonic endothelium and identifies *Scl* as a master regulator of endothelial fate choice.

Developmental fate decisions require precise orchestration of both cell-intrinsic and microenvironmental regulatory mechanisms. Modulation of Wnt signaling has pivotal effects at multiple stages of cardiac mesoderm and progenitor cell development: Wnt antagonists induce cardiac specification from mesoderm and promote cardiomyocyte differentiation (Schneider and Mercola, 2001; Ueno et al., 2007), while activation of canonical Wnt signaling expands cardiac progenitors and maintains them in an undifferentiated state (Qyang et al., 2007). Our study suggests that ectopic cardiomyogenic cells progress through a Wnt-responsive precursor state, the differentiation of which is promoted by Wnt antagonists. Nevertheless, our finding that cardiac conversion was cell intrinsic to loss of *Scl*, and could not be induced solely by secretion of Wnt inhibitors by neighboring *Scl*^{-/-} cells, is in an agreement with the notion that morphogen-induced mesoderm patterning requires relatively uncommitted cells. Recent studies have documented conversion of other mesodermal tissues to cardiomyocytes in vitro and in vivo by reprogramming with a combination of cardiac transcription factors (*Gata4*, *Tbx5*, *Smad3*, and/or *Mef2c*) (Ieda et al., 2010; Qian et al., 2012; Takeuchi and Bruneau, 2009); the same factors were also induced in *Scl*^{-/-} yolk sac endothelial cells. Our data document that an altered cell-intrinsic regulatory program caused by loss *Scl* is sufficient to override the microenvironmental cues that dictate mesodermal fate.

Based on the localization of the CD31⁺Pdgfra⁺ in OFT and AVC in normal hearts, their gene expression (cardiac transcription factors and genes related to EMT) and endothelial origin, we proposed that these cells represent cushion mesenchymal cells, which give rise to the septa and valves (Yamagishi et al., 2009). Thus, our data not only identify markers to enrich putative cushion mesenchymal cells, but also uncover a requirement for *Scl* to suppress cardiomyocyte differentiation in this endothelial-derived precursor. Moreover, analysis of *Isl1*^{-/-} embryos revealed a role for *Isl1* in CD31⁺Pdgfra⁺ cushion mesenchymal cells. As *Isl1* is required for the development of both the multipotent cardiac progenitors and CD31⁺Pdgfra⁺ cushion mesenchymal cells, it was surprising that the ectopic CD31⁺Pdgfra⁺ cells in *Scl*^{-/-} yolk sacs or hearts were not dependent on *Isl1* for their generation. These data indicate that, despite a similar surface phenotype, the CD31⁺Pdgfra⁺ cells in control hearts and *Scl*^{-/-} tissues represent different cells with distinct developmental potential, localization, and regulation. Our data suggests that loss of *Scl* triggers a rapid differentiation program in the endothelium/endocardium that makes ectopic cardiogenesis independent of *Isl1*.

This work has revealed a broader than anticipated potential for embryonic endothelium as a prospective source of multiple mesodermal stem/progenitor cells, introducing the concept of “cardiogenic endothelium.” Our data revealed that endothelium with cardiomyogenic potential emerges in *Scl*^{-/-} embryos in both hemogenic tissues as well as the heart, but not in nonhemogenic head endothelium, implying specificity of latent cardiogenic potential to a unique subset of endothelium. Furthermore, our finding about the distinct temporal windows when cardiogenic fate can be induced in hemogenic endothelium, endocardium, or CD31⁺Pdgfra⁺ putative cushion mesenchymal cells opens up important future questions to define the mechanisms that close the window of opportunity for cardiomyocyte development in different tissues. These data also raise the questions of to what extent can endothelial-derived cardiac cells contribute to normal heart development or regeneration, and how could modulation of *Scl* expression be exploited to improve the differentiation of pluripotent stem cells or partially committed precursors for therapeutic applications. These results call for future studies to examine the prospect of harnessing the latent cardiogenic potential in the vasculature for use in regenerative medicine and to investigate whether similar developmental plasticity exists in other major cell fate decisions in the developing embryo.

EXPERIMENTAL PROCEDURES

Mouse Models

Details about mouse models and genotyping can be found in [Extended Experimental Procedures](#). Mice were maintained according to the guidelines of the University of California, Los Angeles (UCLA), Animal Research Committee.

(D) Gene expression analysis of *Scl*^{-/-} and control CD31⁺Pdgfra⁺ endocardial cells. Differentially expressed (>1.5-fold, $p < 0.05$) cardiac TFs and other proteins and their fold changes, as well as selected GO categories enriched in *Scl*^{-/-} CD31⁺Pdgfra⁺ cells, are shown.

(E) Gene expression analysis of *Scl*^{-/-} and control CD31⁺Pdgfra⁺ cells from the heart. Differentially expressed (>1.5-fold, $p < 0.05$) cardiac TFs and other proteins and their fold changes, as well as selected GO categories enriched in *Scl*^{-/-} CD31⁺Pdgfra⁺ cells, are shown.

(F) IF for Troponin T on cells derived from E 8.5 *Scl*^{-/-} CD31⁺Pdgfra⁺/CD31⁺Pdgfra⁺ cells that were sorted and cultured. Scale bar, 25 μm . See also [Figures S3](#) and [S4](#), [Table S4](#), and [Movies S3](#) and [S4](#).

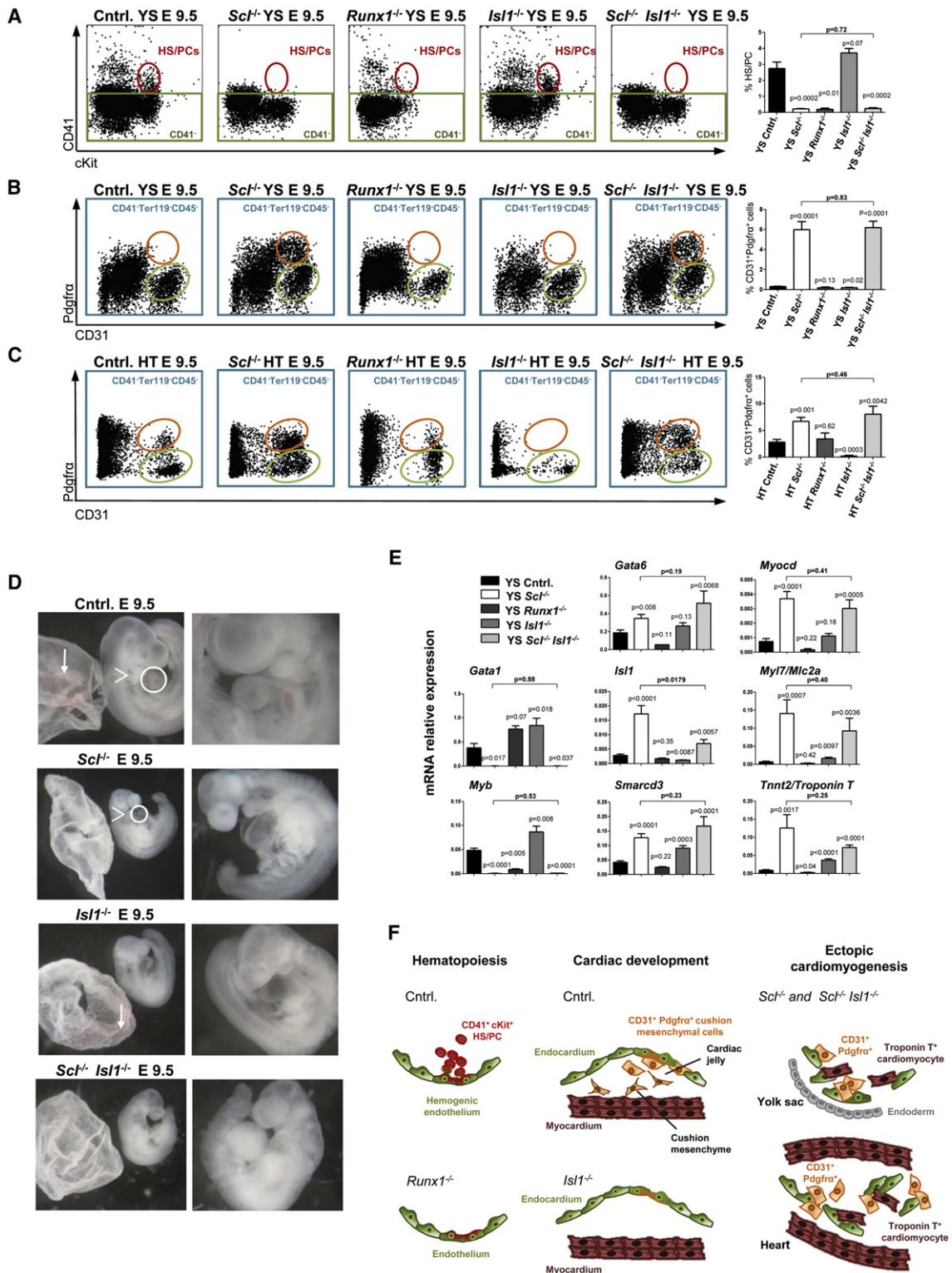


Figure 6. Runx1 and Isl1 Are Not Major Regulators of the Ectopic Cardiomyogenic Cells

(A–C) FACS was performed on (A and B) YS and (C) hearts isolated from control, *Scf*^{-/-}, *Runx1*^{-/-}, *Isl1*^{-/-}, and *Scf*^{-/-} *Isl1*^{-/-} embryos. All p values shown are with respect to control unless otherwise indicated. (A) CD41⁺cKit⁺ HS/PCs (red ovals) are shown in YS and CD31⁺Pdgfra⁺ cells (orange ovals) are shown in (B) YS and (C) heart.

(D) *Scf*^{-/-} *Isl1*^{-/-} embryos lacked blood in the YS (arrows, left panels), pharyngeal arches (arrowheads, left panels), and outflow tract (circles, left panels).

FACS Analysis and Isolation of HS/PCs, Endothelial Cells, and Cardiac Cells

Cells from embryonic tissues were isolated as described elsewhere (Rhodes et al., 2008). For details about FACS, see Extended Experimental Procedures.

Differential Gene Expression Analysis

RNA was isolated using the RNeasy Micro kit (QIAGEN), amplified using the NuGEN Pico kit, and hybridized on Affymetrix Mouse Genome 430 2.0 Array GeneChip microarrays (GEO Accession Number GSE27445). For details on how differentially expressed genes were identified, analyzed and verified, see Extended Experimental Procedures.

Analysis of Tissue Sections and Whole Mounts by Confocal Microscopy

Fixed frozen sections were prepared and stained as described elsewhere (Rhodes et al., 2008), with the same antibodies used in FACS, Troponin I (1:400, Santa Cruz) or cardiac Troponin T (1:400, Sigma). Whole mount yolk sacs were prepared as described elsewhere (Ahnfelt-Ronne et al., 2007) and stained for Troponin T. Confocal images were obtained on a Zeiss LSM 510 equipped with 405 nm, 488 nm, 543 nm, and 633 nm lasers. Images were processed with ImageJ software (National Institutes of Health [NIH]).

Cardiac Culture Assays

Yolk sacs were mechanically dissociated by pipetting or enzymatically dissociated, sorted, and plated on OP9 stromal cells in cardiac medium (α -minimum essential medium with 20% fetal bovine serum, 5 ng/ml murine vascular endothelial growth factor, 50 ng/ml human bone morphogenetic protein 4, and 30 ng/ml human basic fibroblast growth factor; Peprotech) or directly on Matrigel and fibronectin-coated chamber slides (BD Biosciences) with or without 1 μ M XAV939 (Wnt antagonist; Sigma), 2 mM LiCl (Wnt agonist), or 2 mM NaCl (control). Videos were taken with a Nikon Diaphot 300 microscope and XY Clone software (Hamilton Thorne Biosciences). Analysis of beating area was performed using VirtualDub software (v1.9.11) and ImageJ (NIH).

Measurement of Calcium Transients

Yolk sacs were cultured on petri dishes (MatTek Corporation) coated with Matrigel in cardiac medium for 9–10 days. Before imaging, explants were loaded with the Ca^{2+} -sensitive dye Fluo-4AM (Molecular Probes) in the presence of Pluronic F-127 (Molecular Probes). Spontaneous transients were imaged on a Zeiss LSM 5 Pascal confocal microscope equipped with a 488 nm laser.

In Vivo Manipulation of Regulation

Sc1 deletion in *Rosa26Cre-ER^{T2}Sc1^{fl/fl}* embryos was induced by Tamoxifen (Sigma Aldrich T5648) or (Z)-4-hydroxytamoxifen (Sigma Aldrich H7094). Tamoxifen was suspended at 100 mg/ml in ethanol and mixed with sesame oil at a final concentration of 10 mg/ml (10% ethanol). Pregnant females were injected i.p. with 125 μ l tamoxifen at the indicated days. Injections of 250 mg/kg NaCl and LiCl (Wnt agonist) were performed as described (Tian et al., 2010).

Statistical Analysis

For statistical analysis, Student's unpaired two-tailed t test was used for all comparisons.

ACCESSION NUMBERS

For all array data, GEO Accession Number GSE27445 is given earlier, within the Experimental Procedures.

SUPPLEMENTAL INFORMATION

Supplemental Information includes Extended Experimental Procedures, four tables, and five movies and can be found with this article online at <http://dx.doi.org/10.1016/j.cell.2012.06.026>.

ACKNOWLEDGMENTS

The authors thank Dr. Joshua Bloomekatz and Dr. Deborah Yelon for critical reading of the manuscript and sharing unpublished data and Guillaume Hagen for preparing the movies. The authors thank the Broad Stem Cell Research Center Flow Cytometry Core for FACS sorting. This work was funded by the California Institute for Regenerative Medicine (CIRM) New Faculty Award, the Eli and Edythe Broad Center of Regenerative Medicine and Stem Cell Research at UCLA Innovation Award and NIH/RO1 (HL097766-01) grants to H.K.A.M. B.V.H. was supported by the Ruth L. Kirschstein National Research Service Award GM07185 and NIH/National Heart, Lung, and Blood Institute Grant T32 HL69766. A.M.-H was supported by successive fellowships from the European Molecular Biology Organisation and the Human Frontier Science Program. R.F. was funded in part by a CIRM grant to S.K.K. C.J.B. was funded by Rubicon Grant 825.10.016 from the Netherlands Organization for Scientific Research. T.O. was supported by the European Union through the European Social Fund (Mobilitas Grant No. MJD284). S.H.O., an Investigator of the Howard Hughes Medical Institute, is supported in part by a Center of Excellence in Molecular Hematology award from the National Institute of Diabetes and Digestive and Kidney Diseases.

B.V.H. and A.M.-H. conducted project design, experimental work, data analysis and interpretation, and manuscript preparation; R.S., R.F., and T.O. performed bioinformatic data analysis and interpretation, as well as manuscript editing; H.N., C.J.B., and J.S. conducted experimental work, data analysis and interpretation, and manuscript editing; Y.W., S.H., and J.Z. conducted experimental work; X.L., J.-N.C., and S.H.O. performed data interpretation and manuscript editing; M.P. performed bioinformatic method design and manuscript editing; S.K.K., S.M.E., and A.N. conducted project design, data interpretation, and manuscript editing; H.K.A.M. conducted project design, data analysis and interpretation, and manuscript preparation.

Received: September 3, 2011

Revised: April 13, 2012

Accepted: June 1, 2012

Published: August 2, 2012

REFERENCES

- Ahnfelt-Ronne, J., Jorgensen, M.C., Hald, J., Madsen, O.D., Serup, P., and Hecksher-Sorensen, J. (2007). An improved method for three-dimensional reconstruction of protein expression patterns in intact mouse and chicken embryos and organs. *J. Histochem. Cytochem.* 55, 925–930.
- Alva, J.A., Zovein, A.C., Monvoisin, A., Murphy, T., Salazar, A., Harvey, N.L., Carmeliet, P., and Iruela-Arispe, M.L. (2006). VE-Cadherin-Cre-recombinase transgenic mouse: a tool for lineage analysis and gene deletion in endothelial cells. *Developmental Dynamics* 235, 759–767.
- Bertrand, J.Y., Giroux, S., Golub, R., Klaine, M., Jalil, A., Boucontet, L., Godin, I., and Cumano, A. (2005). Characterization of purified intraembryonic hematopoietic stem cells as a tool to define their site of origin. *Proc. Natl. Acad. Sci. USA* 102, 134–139.
- Bertrand, J.Y., Chi, N.C., Santoso, B., Teng, S., Stainer, D.Y., and Traver, D. (2010). Haematopoietic stem cells derive directly from aortic endothelium during development. *Nature* 464, 108–111.

(E) qPCR for hematopoietic and cardiac TFs and cardiomyocyte structural genes on E 9.5 unfractionated YSs; at least two (*Runx1*^{-/-} = 2; all others \geq 5) biological replicates normalized to *HPRT* are shown.

(F) *Runx1* and *Isl1* are required for HS/PC generation and cardiac cushion development, respectively; however, neither regulates ectopic cardiogenesis. In all panels, error bars represent SEM.

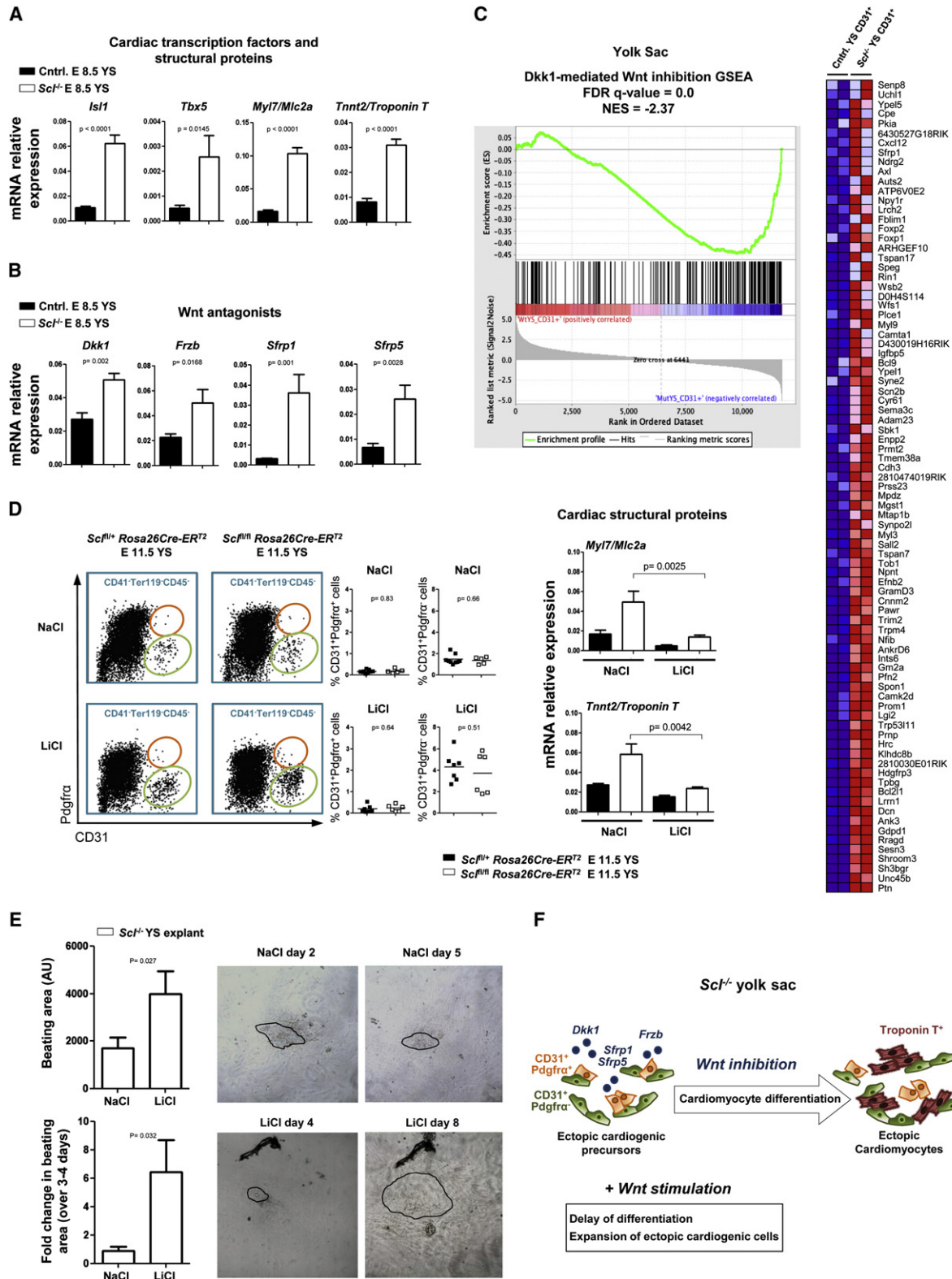


Figure 7. *Scf*^{-/-} Endothelium Expresses and Responds to Wnt Antagonists that Promote Cardiomyocyte Differentiation

(A and B) qPCR for cardiac TFs and cardiomyocyte structural genes (A) and Wnt antagonists on E 8.5 unfractionated YSs (B); four biological replicates normalized to *HPRT* are shown.

- Boisset, J.C., van Cappellen, W., Andrieu-Soler, C., Galjart, N., Dzierzak, E., and Robin, C. (2010). In vivo imaging of haematopoietic cells emerging from the mouse aortic endothelium. *Nature* *464*, 116–120.
- Cai, C.L., Liang, X., Shi, Y., Chu, P.H., Pfaff, S.L., Chen, J., and Evans, S. (2003). Isl1 identifies a cardiac progenitor population that proliferates prior to differentiation and contributes a majority of cells to the heart. *Dev. Cell* *5*, 877–889.
- Chen, M.J., Yokomizo, T., Zeigler, B.M., Dzierzak, E., and Speck, N.A. (2009). Runx1 is required for the endothelial to haematopoietic cell transition but not thereafter. *Nature* *457*, 887–891.
- David, R., Brenner, C., Stieber, J., Schwarz, F., Brunner, S., Vollmer, M., Mentele, E., Muller-Hocker, J., Kitajima, S., Lickert, H., et al. (2008). MesP1 drives vertebrate cardiovascular differentiation through Dkk-1-mediated blockade of Wnt-signalling. *Nat. Cell Biol.* *10*, 338–345.
- de Lange, F.J., Moorman, A.F., Anderson, R.H., Manner, J., Soufan, A.T., de Gier-de Vries, C., Schneider, M.D., Webb, S., van den Hoff, M.J., and Christoffels, V.M. (2004). Lineage and morphogenetic analysis of the cardiac valves. *Circ. Res.* *95*, 645–654.
- Eilken, H.M., Nishikawa, S., and Schroeder, T. (2009). Continuous single-cell imaging of blood generation from haemogenic endothelium. *Nature* *457*, 896–900.
- Fehling, H.J., Lacaud, G., Kubo, A., Kennedy, M., Robertson, S., Keller, G., and Kouskoff, V. (2003). Tracking mesoderm induction and its specification to the hemangioblast during embryonic stem cell differentiation. *Development* *130*, 4217–4227.
- Ieda, M., Fu, J.D., Delgado-Olguin, P., Vedantham, V., Hayashi, Y., Bruneau, B.G., and Srivastava, D. (2010). Direct reprogramming of fibroblasts into functional cardiomyocytes by defined factors. *Cell* *142*, 375–386.
- Ismailoglu, I., Yeaman, G., Daley, G.Q., Perlingeiro, R.C., and Kyba, M. (2008). Mesodermal patterning activity of SCL. *Exp. Hematol.* *36*, 1593–1603.
- Jaspard, B., Couffignal, T., Dufourcq, P., Moreau, C., and Duplaa, C. (2000). Expression pattern of mouse sFRP-1 and mWnt-8 gene during heart morphogenesis. *Mech. Dev.* *90*, 263–267.
- Kassouf, M.T., Hughes, J.R., Taylor, S., McGowan, S.J., Soneji, S., Green, A.L., Vyas, P., and Porcher, C. (2010). Genome-wide identification of TAL1's functional targets: insights into its mechanisms of action in primary erythroid cells. *Genome Res.* *20*, 1064–1083.
- Kattman, S.J., Huber, T.L., and Keller, G.M. (2006). Multipotent flk-1+ cardiovascular progenitor cells give rise to the cardiomyocyte, endothelial, and vascular smooth muscle lineages. *Dev. Cell* *11*, 723–732.
- Kattman, S.J., Witty, A.D., Gagliardi, M., Dubois, N.C., Niapour, M., Hotta, A., Ellis, J., and Keller, G. (2011). Stage-specific optimization of activin/nodal and BMP signaling promotes cardiac differentiation of mouse and human pluripotent stem cell lines. *Cell Stem Cell* *8*, 228–240.
- Kim, I., Saunders, T.L., and Morrison, S.J. (2007). Sox17 dependence distinguishes the transcriptional regulation of fetal from adult hematopoietic stem cells. *Cell* *130*, 470–483.
- Kinder, S.J., Loebel, D.A., and Tam, P.P. (2001). Allocation and early differentiation of cardiovascular progenitors in the mouse embryo. *Trends Cardiovasc. Med.* *11*, 177–184.
- Kissa, K., and Herbomel, P. (2010). Blood stem cells emerge from aortic endothelium by a novel type of cell transition. *Nature* *464*, 112–115.
- Lancrin, C., Sroczynska, P., Stephenson, C., Allen, T., Kouskoff, V., and Lacaud, G. (2009). The haemangioblast generates haematopoietic cells through a haemogenic endothelium stage. *Nature* *457*, 892–895.
- Lindsley, R.C., Gill, J.G., Murphy, T.L., Langer, E.M., Cai, M., Mashayekhi, M., Wang, W., Niwa, N., Nerbonne, J.M., Kyba, M., et al. (2008). Mesp1 coordinately regulates cardiovascular fate restriction and epithelial-mesenchymal transition in differentiating ESCs. *Cell Stem Cell* *3*, 55–68.
- Mikkola, H.K., Fujiwara, Y., Schlaeger, T.M., Traver, D., and Orkin, S.H. (2003a). Expression of CD41 marks the initiation of definitive hematopoiesis in the mouse embryo. *Blood* *101*, 508–516.
- Mikkola, H.K., Klintman, J., Yang, H., Hock, H., Schlaeger, T.M., Fujiwara, Y., and Orkin, S.H. (2003b). Haematopoietic stem cells retain long-term repopulating activity and multipotency in the absence of stem-cell leukaemia SCL/tal-1 gene. *Nature* *421*, 547–551.
- Moretti, A., Caron, L., Nakano, A., Lam, J.T., Bernshausen, A., Chen, Y., Qyang, Y., Bu, L., Sasaki, M., Martin-Puig, S., et al. (2006). Multipotent embryonic isl1+ progenitor cells lead to cardiac, smooth muscle, and endothelial cell diversification. *Cell* *127*, 1151–1165.
- Nostro, M.C., Cheng, X., Keller, G.M., and Gadue, P. (2008). Wnt, activin, and BMP signaling regulate distinct stages in the developmental pathway from embryonic stem cells to blood. *Cell Stem Cell* *2*, 60–71.
- Palencia-Desai, S., Kohli, V., Kang, J., Chi, N.C., Black, B.L., and Sumanas, S. (2011). Vascular endothelial and endocardial progenitors differentiate as cardiomyocytes in the absence of Etsrp/Etv2 function. *Development* *138*, 4721–4732.
- Park, I.K., Qian, D., Kiel, M., Becker, M.W., Pihalja, M., Weissman, I.L., Morrison, S.J., and Clarke, M.F. (2003). Bmi-1 is required for maintenance of adult self-renewing haematopoietic stem cells. *Nature* *423*, 302–305.
- Qian, L., Huang, Y., Spencer, C.I., Foley, A., Vedantham, V., Liu, L., Conway, S.J., Fu, J.D., and Srivastava, D. (2012). In vivo reprogramming of murine cardiac fibroblasts into induced cardiomyocytes. *Nature* *485*, 593–598.
- Qyang, Y., Martin-Puig, S., Chiravuri, M., Chen, S., Xu, H., Bu, L., Jiang, X., Lin, L., Granger, A., Moretti, A., et al. (2007). The renewal and differentiation of Isl1+ cardiovascular progenitors are controlled by a Wnt/beta-catenin pathway. *Cell Stem Cell* *1*, 165–179.
- Rasmussen, T.L., Kweon, J., Diekmann, M.A., Belema-Bedada, F., Song, Q., Bowlin, K., Shi, X., Ferdous, A., Li, T., Kyba, M., et al. (2011). ER71 directs mesodermal fate decisions during embryogenesis. *Development* *138*, 4801–4812.
- Rhodes, K.E., Gekas, C., Wang, Y., Lux, C.T., Francis, C.S., Chan, D.N., Conway, S., Orkin, S.H., Yoder, M.C., and Mikkola, H.K. (2008). The emergence of hematopoietic stem cells is initiated in the placental vasculature in the absence of circulation. *Cell Stem Cell* *2*, 252–263.
- Schlaeger, T.M., Mikkola, H.K., Gekas, C., Helgadottir, H.B., and Orkin, S.H. (2005). Tie2Cre-mediated gene ablation defines the stem-cell leukemia gene (SCL/tal1)-dependent window during hematopoietic stem-cell development. *Blood* *105*, 3871–3874.
- Schneider, V.A., and Mercola, M. (2001). Wnt antagonism initiates cardiogenesis in *Xenopus laevis*. *Genes Dev.* *15*, 304–315.
- Schoenebeck, J.J., Keegan, B.R., and Yelon, D. (2007). Vessel and blood specification override cardiac potential in anterior mesoderm. *Dev. Cell* *13*, 254–267.

(C) GSEA of expression data from E 9.25 *Scf*^{-/-} and control YS CD31⁺ cells compared to embryoid bodies treated with the Wnt antagonist Dkk1. The heat map depicts genes that are part of the core enrichment set. The false discovery rate (FDR) q value and normalized enrichment score (NES) are shown.

(D) Pregnant dams were injected with tamoxifen on E 6.5 and treated daily with either NaCl (control) or LiCl (Wnt agonist). FACS analysis showing the frequency of CD31⁺Pdgfr α ⁻ and CD31⁺Pdgfr α ⁺ cells after NaCl or LiCl treatment and qPCR for *Myl7* and *Tnnt2*.

(E) *Scf*^{-/-} YSs were cultured with either NaCl or LiCl; videos of beating clusters were taken and the area measured in arbitrary units (AU; n \geq 27). Explants were imaged at two time points during the culture period (n \geq 3); beating areas are outlined.

(F) Schematic depicting the acceleration of differentiation of ectopic cardiogenic cells by Wnt inhibitors derived from *Scf*^{-/-} endothelium; this could be attenuated by the Wnt agonist LiCl. In all panels, error bars represent SEM.

See also Figure S5 and Movie S5.

- Shivdasani, R.A., Mayer, E.L., and Orkin, S.H. (1995). Absence of blood formation in mice lacking the T-cell leukaemia oncoprotein tal-1/SCL. *Nature* *373*, 432–434.
- Simões, F.C., Peterkin, T., and Patient, R. (2011). Fgf differentially controls cross-antagonism between cardiac and haemangioblast regulators. *Development* *138*, 3235–3245.
- Souroullas, G.P., Salmon, J.M., Sablitzky, F., Curtis, D.J., and Goodell, M.A. (2009). Adult hematopoietic stem and progenitor cells require either Lyl1 or Scf for survival. *Cell Stem Cell* *4*, 180–186.
- Stadtfeld, M., and Graf, T. (2005). Assessing the role of hematopoietic plasticity for endothelial and hepatocyte development by non-invasive lineage tracing. *Development* *132*, 203–213.
- Takeuchi, J.K., and Bruneau, B.G. (2009). Directed transdifferentiation of mouse mesoderm to heart tissue by defined factors. *Nature* *459*, 708–711.
- Tian, Y., Yuan, L., Goss, A.M., Wang, T., Yang, J., Lepore, J.J., Zhou, D., Schwartz, R.J., Patel, V., Cohen, E.D., et al. (2010). Characterization and in vivo pharmacological rescue of a Wnt2-Gata6 pathway required for cardiac inflow tract development. *Dev. Cell* *18*, 275–287.
- Ueno, S., Weidinger, G., Osugi, T., Kohn, A.D., Golob, J.L., Pabon, L., Reinecke, H., Moon, R.T., and Murry, C.E. (2007). Biphasic role for Wnt/ beta-catenin signaling in cardiac specification in zebrafish and embryonic stem cells. *Proc. Natl. Acad. Sci. USA* *104*, 9685–9690.
- Visvader, J.E., Fujiwara, Y., and Orkin, S.H. (1998). Unsuspected role for the T-cell leukemia protein SCL/tal-1 in vascular development. *Genes Dev.* *12*, 473–479.
- Wilson, N.K., Foster, S.D., Wang, X., Knezevic, K., Schutte, J., Kaimakis, P., Chilarska, P.M., Kinston, S., Ouwehand, W.H., Dzierzak, E., et al. (2010). Combinatorial transcriptional control in blood stem/progenitor cells: genome-wide analysis of ten major transcriptional regulators. *Cell Stem Cell* *7*, 532–544.
- Yamagishi, T., Ando, K., and Nakamura, H. (2009). Roles of TGFbeta and BMP during valvulo-septal endocardial cushion formation. *Anat. Sci. Int.* *84*, 77–87.
- Zeigler, B.M., Sugiyama, D., Chen, M., Guo, Y., Downs, K.M., and Speck, N.A. (2006). The allantois and chorion, when isolated before circulation or chorio-allantoic fusion, have hematopoietic potential. *Development* *133*, 4183–4192.
- Zovein, A.C., Hofmann, J.J., Lynch, M., French, W.J., Turlo, K.A., Yang, Y., Becker, M.S., Zanetta, L., Dejana, E., Gasson, J.C., et al. (2008). Fate tracing reveals the endothelial origin of hematopoietic stem cells. *Cell Stem Cell* *3*, 625–636.